

Loss of the Parkinson's disease-linked gene DJ-1 perturbs mitochondrial dynamics

I. Irrcher¹, H. Aleyasin¹, E.L. Seifert², S.J. Hewitt¹, S. Chhabra¹, M. Phillips¹, A.K. Lutz⁴, M.W.C. Rousseaux¹, L. Bevilacqua², A. Jahani-Asl¹, S. Callaghan¹, J.G. MacLaurin¹, K.F. Winklhofer⁴, P. Rizzu⁵, P. Rippstein³, R.H. Kim⁶, C.X. Chen⁷, E.A. Fon⁷, R.S. Slack¹, M.E. Harper², H.M. McBride³, T.W. Mak⁶ and D.S. Park^{1,8,*}

¹Department of Cellular and Molecular Medicine, ²Department of Biochemistry, Microbiology, and Immunology and ³Ottawa Heart Institute, University of Ottawa, Ottawa, Canada, ⁴Adolf Butenandt Institute, Neurobiochemistry, Ludwig Maximilians University, Munich, Germany, ⁵Department of Clinical Genetics, Medical Genomics VU University Medical Center, Amsterdam, The Netherlands, ⁶The Campbell Family Institute for Breast Cancer Research, University of Toronto, Toronto, Canada, ⁷Department of Biochemistry, McGill University, Montreal, Canada and ⁸Department of Cogno-Mechatronics Engineering, Pusan National University, Korea

Received June 2, 2010; Revised and Accepted July 7, 2010

Growing evidence highlights a role for mitochondrial dysfunction and oxidative stress as underlying contributors to Parkinson's disease (PD) pathogenesis. DJ-1 (PARK7) is a recently identified recessive familial PD gene. Its loss leads to increased susceptibility of neurons to oxidative stress and death. However, its mechanism of action is not fully understood. Presently, we report that DJ-1 deficiency in cell lines, cultured neurons, mouse brain and lymphoblast cells derived from DJ-1 patients display aberrant mitochondrial morphology. We also show that these DJ-1-dependent mitochondrial defects contribute to oxidative stress-induced sensitivity to cell death since reversal of this fragmented mitochondrial phenotype abrogates neuronal cell death. Reactive oxygen species (ROS) appear to play a critical role in the observed defects, as ROS scavengers rescue the phenotype and mitochondria isolated from DJ-1 deficient animals produce more ROS compared with control. Importantly, the aberrant mitochondrial phenotype can be rescued by the expression of Pink1 and Parkin, two PD-linked genes involved in regulating mitochondrial dynamics and quality control. Finally, we show that DJ-1 deficiency leads to altered autophagy in murine and human cells. Our findings define a mechanism by which the DJ-1-dependent mitochondrial defects contribute to the increased sensitivity to oxidative stress-induced cell death that has been previously reported.

INTRODUCTION

Parkinson's disease (PD), the second most common neurodegenerative disorder, is characterized by the progressive loss of neurons within the substantia nigra *pars compacta* (1,2). Though the pathogenic mechanisms underlying PD are not well understood, growing evidence supports a role for mitochondrial dysfunction, oxidative stress and more recently autophagy.

Mitochondrial dysfunction was initially tied to PD in studies demonstrating the presence of aberrant mitochondrial function in idiopathic PD patients (3,4). Moreover, several dopamin-

ergic toxins acted as mitochondrial toxins by inhibiting the electron transport chain, producing toxic-free radicals in the process (5,6). Since this time, several familial PD genes, including, Parkin (PARK2), Pink1 (PARK6) and DJ-1 (PARK7), have been linked to mitochondria. Their loss results in abnormal mitochondrial morphology (7,8). Interestingly, the interplay of Pink1 and Parkin dynamically regulates mitochondrial morphology via mitochondrial fission/fusion and also affects mitochondrial quality control (9–11). As the function of Pink1 and Parkin in these contexts continues to be elucidated, the role(s) of DJ-1 is less understood.

*To whom correspondence should be addressed at: Faculty of Medicine, Department Of Cellular and Molecular Medicine (CMM), University of Ottawa, 451 Smyth Road, Ottawa, Ontario, Canada K1H 8M5. Tel: +1 6135625800 ext. 8816; Fax: +1 6135625403; Email: dpark@uottawa.ca

Homozygous loss-of-function mutations in DJ-1 (PARK7) result in early onset PD (12). Several lines of evidence, including our own, indicate that DJ-1 protects neurons against oxidative stress-induced cell death (13,14). It has been postulated that DJ-1 exerts its protective function by regulating mitochondrial homeostasis or participating in the oxidative stress response either serving as an antioxidant scavenger or a redox sensor (14–17). More recently, DJ-1 was found to affect mitochondrial quality control (18,19). Given the importance of reactive oxygen species (ROS) in regulating mitochondrial dynamics and the observations that loss of Pink1 and Parkin has also been linked to mitochondrial dysfunction, we wanted to address whether DJ-1 also affects mitochondrial dynamics and function.

Here we examined mitochondrial morphology and function in DJ-1 deficient tissues and hypothesized that loss of DJ-1 would produce a fragmented mitochondrial phenotype, accounting increased sensitivity to cell death of DJ-1 deficient neurons previously reported (14). We demonstrate that DJ-1 deficiency leads to a fragmented mitochondrial phenotype in multiple contexts including neurons and human DJ-1 patient cells. Second, we provide evidence that ROS plays a critical role in this fragmentation phenotype and that DJ-1 deficiency results in elevated ROS levels. Third, we show that this mitochondrial phenotype is an important contributor to the sensitivity to oxidative stress caused by the loss of DJ-1. Fourth, we show that Pink1 and Parkin can rescue the mitochondrial fragmentation induced by the loss of DJ-1. Finally, we also show that the loss of DJ-1 results in increased autophagic activity.

RESULTS

Loss of DJ-1 alters mitochondrial morphology and dynamics

Based upon the growing evidence for mitochondrial morphology and dynamics as underlying contributors to PD, we first investigated a role for DJ-1 in mitochondrial remodeling. Primary cortical neurons and mouse embryonic fibroblasts (MEFs) from DJ-1^{+/+} or DJ-1^{-/-} embryos (E15.5) were cultured. Mitochondria were quantified and binned according to length, as done previously (20). As shown in Figure 1A and quantified in Figure 1B, mitochondrial lengths in DJ-1^{+/+} primary cortical neurons at 3 days *in vitro* were significantly longer and less fragmented than in DJ-1^{-/-} neurons. This fragmented mitochondrial phenotype was also evident in MEFs (Fig. 1C and D) and *in vivo* in the striatum of DJ-1^{+/+} and DJ-1^{-/-} mice (Fig. 1E and F). Thus, the fragmented morphology appears to be a more generalized phenomenon rather than restricted to a specific cell type, occurring both *in vitro* and *in vivo*. These data demonstrate that mitochondrial morphology is altered with the loss of DJ-1.

To address whether the DJ-1-dependent mitochondrial fragmentation was related to alterations in mitochondrial fusion rates, DJ-1^{+/+} or DJ-1^{-/-} MEFs were transduced with a matrix-targeted photoactivatable GFP lentivirus (PA-GFP). PA-GFP was activated in ~10% of the cell using a 405 nm laser line at 75% intensity (21). Upon photoactivation, the spread of the GFP signal throughout the mitochondrial reticu-

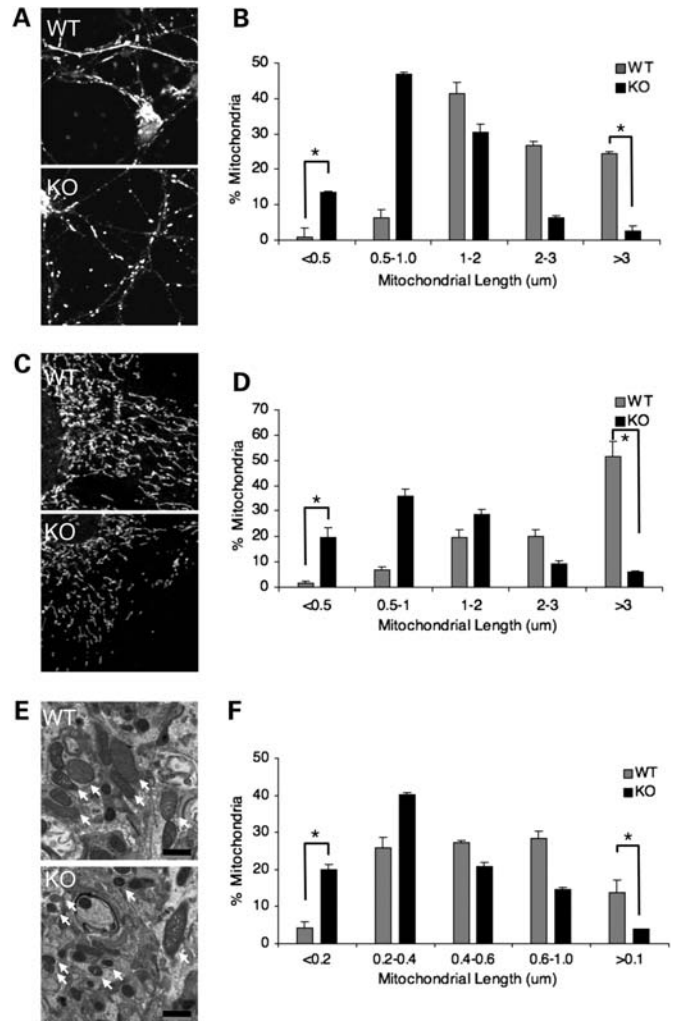


Figure 1. DJ-1 deficiency results in altered mitochondrial morphology *in vitro* and *in vivo*. (A) Primary cortical neurons (3 DIV) and (C) MEFs from wild-type (WT) and knockout (KO) DJ-1 embryos were harvested and fixed as described under Materials and Methods and immunostained with antibodies to Tom20 to visualize mitochondria. Quantification of mitochondrial lengths in (B) primary cortical neurons and (D) MEFs was done as described previously [Jahani-Asl *et al.* (20); $n = 4$ independent experiments with a minimum of 500 mitochondria/experiment counted]. Scale Bar = 2 μm. * $P < 0.05$ versus respective $+/+$ control. (E) Electron microscopic images of WT and KO DJ-1 striatum prepared as described in Materials and Methods. (F) Quantification of mitochondrial diameters in the striatum of WT and KO DJ-1 mice from three mice/genotype. Scale bar = 500 nm. * $P < 0.05$ versus respective WT DJ-1 control. DIV, days *in vitro*. White arrows in (E) depict mitochondria.

lum was assessed immediately post-activation and following 20 min (Fig. 2A). The data in Figure 2B demonstrate that mitochondrial fusion in MEFs is decreased by 30% DJ-1^{-/-} when compared with DJ-1^{+/+}. Steady-state levels of the mitochondrial fission and fusion proteins, Dynamin Related Protein-1 (Drp1) and mitofusin 1 (MFN1) were also measured to determine whether the loss of DJ-1 would result in altered expression. As shown in Figure 2C, Drp1 levels were not altered, while decreases in the levels of MFN1 were observed.

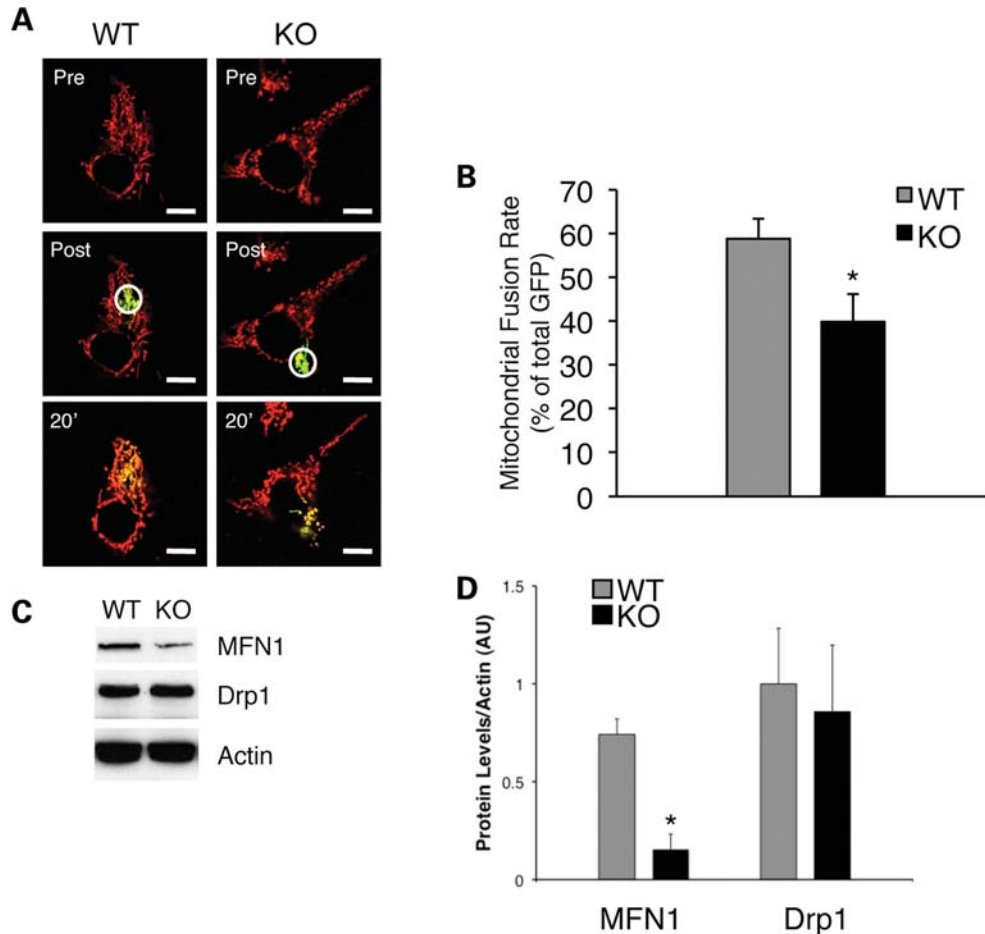


Figure 2. Mitochondrial fusion is decreased with DJ-1 deficiency. (A) Confocal images of mitochondria from DJ-1^{+/+} (WT) and DJ-1^{-/-} (KO) MEFs transduced with mitochondrial matrix-targeted DS-red and PA-GFP lentiviruses as described in the Supplementary Information. Images shown are from pre-activation (Pre), immediately following activation (Post) in a small region of interest (indicated by open white circles) as well as following 20 min (20') of activation. (B) Quantification of mitochondrial fusion 20 min post-activation from DJ-1^{+/+} ($n = 14$ cells) and DJ-1^{-/-} ($n = 12$ cells) MEFs. (C) Protein extracts were made from DJ-1^{+/+} and DJ-1^{-/-} MEFs and subjected to western blotting for Drp-1, Mfn1 and actin (for loading control). Data shown are representative of at least three independent experiments. (D) Quantification of Drp1 and MFN1 protein levels, corrected with actin for loading in DJ-1 WT and KO MEFs. * $P < 0.05$.

Rescue of mitochondrial length in DJ-1^{-/-} neurons abrogates neuronal cell death

Our previous work has shown that overexpression of DJ-1 protects primary cortical neurons from oxidative stress (14). Here we report that DJ-1 deficiency promotes mitochondrial fragmentation. To determine whether these phenomena are linked, primary cortical neurons from DJ-1^{+/+} and DJ-1^{-/-} embryos were infected with dominant-negative dynamin-related protein 1 (DRP1K38E), a mutant form of the mitochondrial fission factor that promotes an elongated mitochondrial reticulum when expressed in cells. Expression levels of Drp1 K38E are shown in Figure 3A and were previously described (21). When primary cortical neurons were subjected to oxidative stress in the form of MPP⁺ (10 μ M), a metabolite of the parkinsonism-inducing drug MPTP (22) for 48 h, the hypersensitive DJ-1^{-/-} neurons showed an increase in cell death. However, DJ-1^{-/-} cortical neurons infected with DRP1K38E were completely protected from the toxic effects of MPP⁺ suggesting that mitochondrial fragmentation contributes to oxidative stress-induced sensitivity to cell death (Fig. 3B).

NAC treatment rescues the mitochondrial phenotype in DJ-1^{-/-} neurons

ROS can significantly influence mitochondrial morphology, producing a fragmented phenotype (23). Thus, to assess whether the DJ-1-dependent mitochondrial morphology is related to ROS, we determined whether quenching with N-acetyl-L-cysteine (NAC) might affect mitochondrial fragmentation observed in DJ-1 deficient cells. DJ-1^{+/+} and DJ-1^{-/-} primary cortical neurons were incubated with the ROS scavenger NAC (1 mM) for 48 h (Fig. 4A). Quantification of mitochondrial lengths in vehicle-treated (VEH) DJ-1^{+/+} and DJ-1^{-/-} neurons revealed a similar pattern of mitochondrial morphology deficits as described in Figure 1. While treatment with NAC did not significantly alter mitochondrial length in the DJ-1^{+/+} neurons, treatment of DJ-1^{-/-} neurons with NAC completely reversed the mitochondrial fragmentation where the percentage of mitochondria exhibiting lengths greater than 3 μ m increased (i.e. $1.14 \pm 0.305\%$ in KO-VEH to $32.144 \pm 3.141\%$ in KO-NAC; Fig. 2B) and the percentage of fragmented mitochondria decreased (i.e.

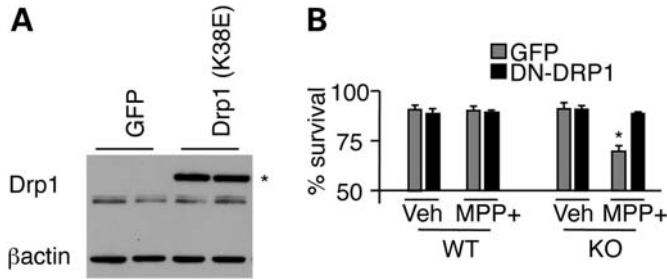


Figure 3. Mitochondrial length is critical for neuronal cell survival. (A) Primary cortical neurons infected with either GFP or DN-Drp1 were treated with vehicle (Veh) or MPP+ (10 μ M) for 24 h. (B) Cell survival was assessed by counting infected cells with intact or dead nuclei plotting the ratio of live:dead cells in treated and untreated DJ-1^{+/+} and DJ-1^{-/-} ($n = 3$ independent experiments, each experiment was performed in triplicate).

<0.5 μ m; $15.928 \pm 3.03\%$ in KO-VEH versus $0.198 \pm 0.038\%$ in KO-NAC; Fig. 4B), suggesting that elevated levels of ROS can cause mitochondrial fragmentation, which can be reversed if ROS levels are reduced.

Wild-type DJ-1 but not the DJ-1 C106A mutant rescue mitochondrial morphology defects

It has been previously reported that DJ-1 exerts its effect on oxidative stress via an isoelectric pH shift resulting in a more acidic molecule (24). Importantly, the residue that appears to be sensitive to oxidative modification, in particular hydrogen peroxide-induced oxidation, is a cysteine residue in position 106 (25,26). Thus, to provide additional relevance for the role of ROS and the importance of DJ-1 and oxidative stress in the regulation of mitochondrial morphology, we investigated whether DJ-1 itself actively regulates mitochondrial morphology and to further ascertain whether the DJ-1 mutant that is defective in handling ROS would fail to rescue the DJ-1 deficient phenotype. DJ-1^{+/+} and DJ-1^{-/-} cortical neurons were infected with adenoviruses encoding GFP (as a control), wild-type DJ-1 (DJ-1) or an oxidant mutant form of DJ-1 (C106A). This DJ-1 mutant harbors a cysteine to alanine point mutation at amino acid 106 rendering the oxidative capacity of DJ-1 non-functional. Expression levels of viruses are shown in Supplementary Material, Fig. S1. As shown in Figure 5A and quantified in Figure 5B, DJ-1^{+/+} or DJ-1^{-/-} cortical neurons infected with GFP virus alone display the wild-type mitochondrial phenotype as shown in Figure 1, demonstrating that viral expression of GFP alone does not significantly alter mitochondrial length. Next, while overexpression of DJ-1 had no effect on mitochondrial morphology in DJ-1^{+/+} neurons, DJ-1 expression in DJ-1^{-/-} neurons increased the percentage of mitochondria exhibiting lengths greater than 3 μ m ($5.15 \pm 0.826\%$ in KO-GFP versus $47.97 \pm 12.51\%$ in KO DJ-1) and decreased the percentage of fragmented mitochondria ($42.00 \pm 2.56\%$ in KO-GFP versus $1.403 \pm 1.4\%$ in KO DJ-1) supporting the idea that wild-type DJ-1 plays a role in regulating mitochondrial morphology. On the other hand, the oxidant mutant C106A cannot recapitulate the full rescue displayed by WT DJ-1 indicating that the redox function of DJ-1 is critical in promoting a fused mitochondrial reticulum.

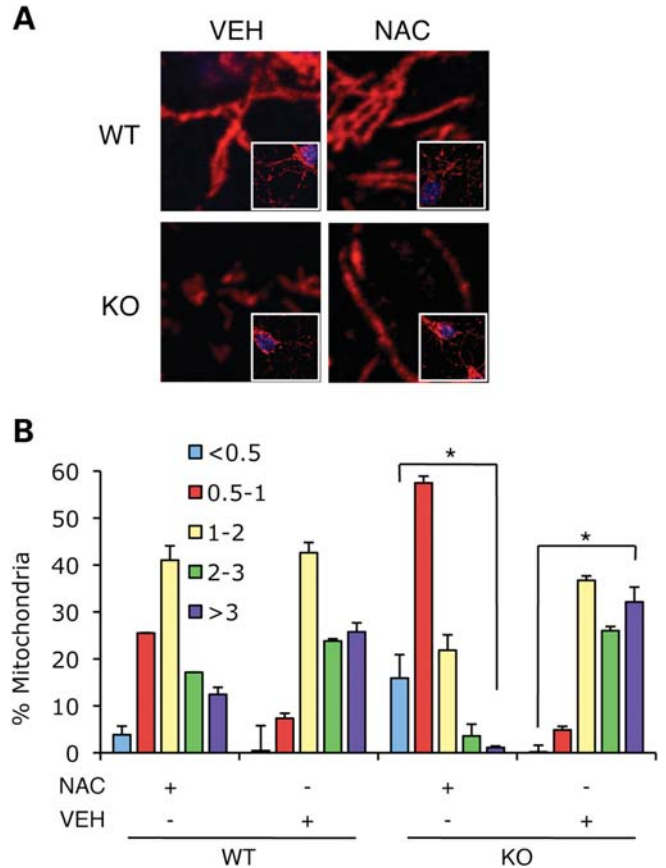


Figure 4. NAC rescues the mitochondrial morphology in DJ-1-deficient primary cortical neurons. (A) Confocal images of neurons taken from vehicle- (VEH) and NAC-treated (NAC) WT and KO neurons. Neurons were harvested and fixed 48 h post-treatment and immunostained with antibodies to Tom20 (red) to visualize mitochondria. Scale bar = 2 μ m. Inset: lower magnification images. (B) Quantification of mitochondrial lengths as described previously [Jahani-Asl *et al.* (20); $n = 3$ independent experiments with a minimum of 500 mitochondria/experiment were counted]. Scale bar = 2 μ m. * $P < 0.05$ versus respective controls.

DJ-1 deficiency alters ROS production

If ROS were indeed important in promoting the fragmented mitochondrial phenotype induced by DJ-1 deficiency, we would expect that ROS production would be elevated in mitochondria isolated from DJ-1^{-/-} mice when compared with DJ-1^{+/+} controls. Accordingly, we isolated mitochondrial fractions from brain and skeletal muscle; tissues typically associated with high metabolic requirements and mitochondria and are therefore significant sources of ROS. As predicted, we observed that H₂O₂ production in mitochondria isolated from DJ-1^{-/-} mice is increased 1.4-fold ($P < 0.05$) compared with DJ-1^{+/+} controls in both brain (Fig. 6) and skeletal muscle (Supplementary Material, Fig. S2A), respectively. In either tissue, H₂O₂ production in the DJ-1^{-/-} animals was not further increased with the addition of the mitochondrial Complex I inhibitor rotenone, suggesting that ROS production in DJ-1 deficient mitochondria is generated primarily via Complex I. Despite the increased H₂O₂ production, we did not observe gross differences in mitochondrial function

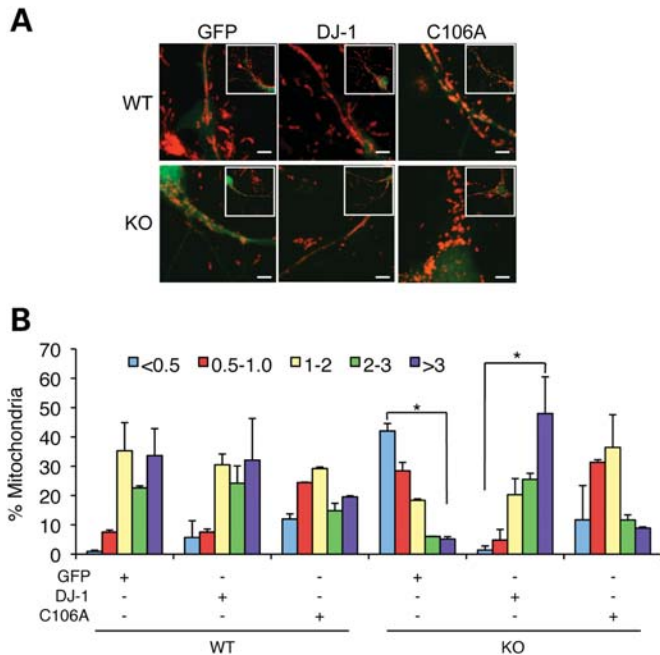


Figure 5. Restoration of wild-type mitochondrial phenotype upon re-expression of DJ-1 *in vitro*. (A) Confocal images from WT and KO DJ-1 primary cortical neurons infected with GFP, GFP-DJ-1 and GFP-DJ-1 C106A adenoviruses as described in Materials and Methods. Neurons were harvested and fixed 48 h post-infection and immunostained with antibodies to Tom20 (red) to visualize mitochondria. Inset: lower magnification images. (B) Quantification of mitochondrial lengths as described previously [Jahani-Asl *et al.* (20); $n = 3$ independent experiments with a minimum of 500 mitochondria/experiment that were counted per condition]. * $P < 0.05$ versus respective controls.

measurements that were performed such as mitochondrial respiration and citrate synthase activity in DJ-1^{-/-} mice, at least in the brain (Supplementary Material, Fig. S2B and S2C). However, it should be noted that both mitochondrial respiration and citrate synthase activity were decreased in skeletal muscle (Supplementary Material, Fig. S2D and S2E).

Pink1 and Parkin rescue mitochondrial length in DJ-1^{-/-} primary cortical neurons

Previous work conducted in *Drosophila* has demonstrated that Pink1 and Parkin participate in mitochondrial remodeling and are part of the same genetic pathway where Pink1 is upstream of Parkin (9–11,27–29). More recent evidence in mammalian cells is supportive of this notion and also implicates Parkin and Pink1 in the regulation of autophagy, a lysosomal degradation pathway responsible for the degradation of damaged proteins and organelles, including mitochondria (29–31). Thus, we determined whether Pink1 and Parkin could rescue the mitochondrial phenotype in DJ-1^{-/-} primary cortical neurons. Accordingly, we infected DJ-1^{+/+} and DJ-1^{-/-} primary cortical neurons with Pink1 and Parkin viruses, and quantified mitochondrial length as before. Viral expression of Parkin was confirmed in Supplementary Material, Fig. S3.

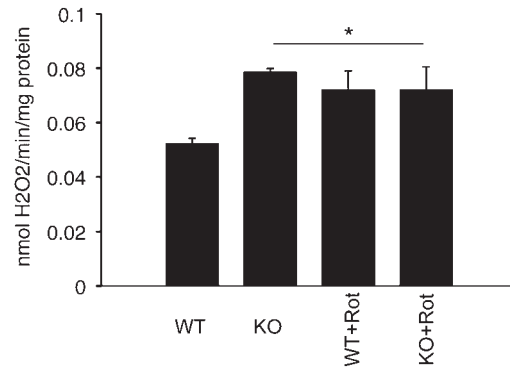


Figure 6. Brain mitochondria isolated from DJ-1 deficient animals produce more ROS. H₂O₂ production was measured in mitochondria isolated from WT and KO DJ-1 brains. * $P < 0.05$ versus WT DJ-1 (P/M, pyruvate/malate; Rot, rotenone).

Viral expression of Pink1 was previously described (32). As shown in Figure 7A and C and quantified in Figure 7B and D, overexpression of either Pink1 or Parkin in DJ-1^{-/-} primary cortical neurons promoted an increase in the percentage of mitochondria that were greater than 3 μm in length ($5.151 \pm 0.826\%$ in KO-GFP versus $44.08 \pm 1.646\%$ in KO-Pink1; Fig. 7B and $1.686 \pm 0.133\%$ in KO-GFP versus $30.126 \pm 8.068\%$ in KO-Parkin; Fig. 7D) and decreased the percentage of fragmented mitochondria (i.e. $<0.5 \mu\text{m}$; $42.00 \pm 2.562\%$; Fig. 7B in KO-GFP versus $0.948 \pm .271\%$ in KO-Pink1 and $34.108 \pm 5.50\%$ in KO-GFP versus $4.888 \pm 2.924\%$ in KO-Parkin; Fig. 7D) respectively, suggesting that both Pink1 and Parkin can rescue the fragmentation phenotype observed with the loss of DJ-1.

To further confirm these findings, we also quantified the percentage of cells that contained fragmented mitochondria a dopaminergic cell line (SH-5Y5Y) in which DJ-1 was transiently knocked down and subsequently overexpressed with Parkin or Pink1. Confirmation of DJ-1, Pink1 and Parkin overexpression is shown in Supplementary Material, Fig. S4A, S4B and S4C, respectively. As seen in DJ-1^{-/-} primary cortical neurons, transient knockdown of DJ-1 produced a significant increase in cells exhibiting fragmented mitochondria and this phenotype could be prevented with overexpression of DJ-1, Pink1 or Parkin (Fig. 7E and F).

DJ-1 deficiency results in enhanced autophagic flux

As mentioned above, Pink1 and Parkin have both been implicated in the regulation of autophagy in response to mitochondrial damage (9–11,30,31). Our present data show that the loss of DJ-1 leads to increased mitochondrial ROS production and fragmentation. Since both of these parameters are linked with autophagy, we evaluated whether a downstream autophagic response might also be altered with DJ-1 deficiency. To this end, we employed conventional autophagy assays including the evaluation of steady-state microtubule-associated protein light chain 3-II (LC3-II) and the LC3-associated protein p62, under basal conditions as well as GFP-LC3 puncta formation (33). As shown in Figure 8A, the markers

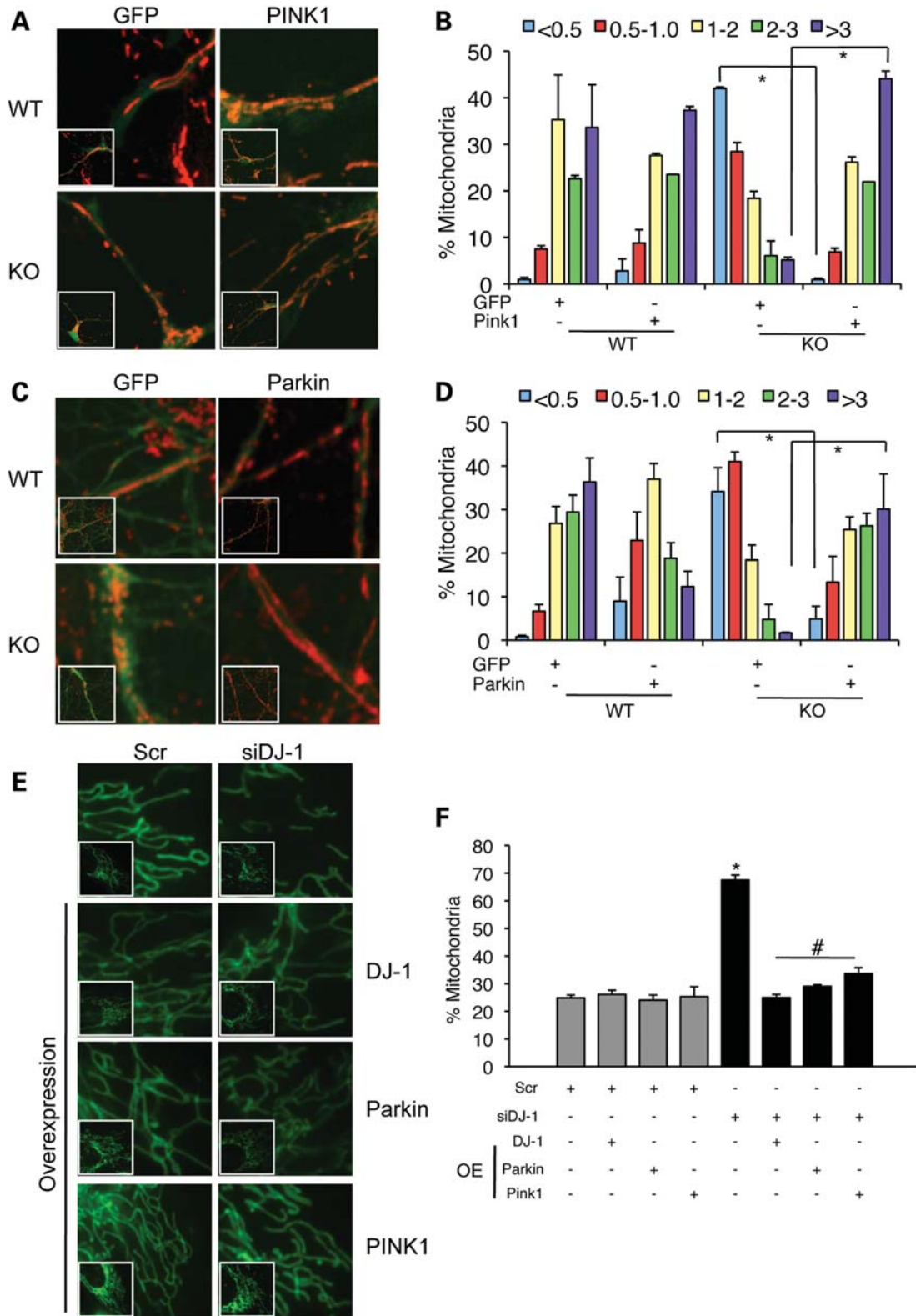


Figure 7. Rescue of mitochondrial morphology with Pink1 and Parkin in a DJ-1-deficient background. (A) Confocal images from WT and KO DJ-1 primary cortical neurons infected with GFP or GFP-PINK1 adenoviruses as described in Materials and Methods. Neurons were harvested and fixed 48 h post-infection and immunostained with antibodies to Tom20 (red) to visualize mitochondria. Inset: lower magnification images. (B) Quantification of mitochondrial lengths as described previously [Jahani-Asl *et al.* (20); $n = 3$ independent experiments with a minimum of 500 mitochondria/experiment that were counted per condition]. Scale bar = 5 μ m. * $P < 0.05$ versus respective controls. (C) Confocal images from WT and KO DJ-1 primary cortical neurons infected with eGFP or eGFP-Parkin adeno-associated viruses as described in Materials and Methods. Neurons were harvested and fixed 4 days post-infection and immunostained with

of autophagy p62 and LC3-II levels in DJ-1^{-/-} mouse embryonic fibroblasts (MEFs) are decreased compared with DJ-1^{+/+} controls, indicating that the loss of DJ-1 results in a reduction in autophagosomes since levels of LC3-II correlate with autophagosome number (34,35). This reduction can either be attributed to the downregulation of autophagosome formation or enhanced autophagic degradation (34). The use of bafilomycin A1, a late inhibitor of autophagy (34), restores steady-state p62 as well as LC3-II protein levels suggesting that the loss of DJ-1 enhances autophagic degradation, in other words autophagic activity is overactive. Next, we made use of the H1299 cell line in which GFP-LC3 is stably expressed and transiently reduced DJ-1 protein levels via siRNA to confirm the DJ-1-dependent perturbations in the autophagic pathway. As shown in Figure 8B, at 48 h post-transfection, the level of DJ-1 was significantly reduced upon transfection of a siRNA specifically targeted to DJ-1. The effect of DJ-1 knockdown was accompanied by a significant decrease in p62 levels, and an increased accumulation of cleaved GFP demonstrating that autophagic activity is enhanced by transient knockdown of DJ-1 (Fig. 8B). This was further observed with immunofluorescence where GFP puncta formation was increased by 1.5-fold ($P < 0.05$) with transient knockdown of DJ-1 (Fig. 8C and D). Given the recent involvement of Parkin and PINK1 in the regulation of mitochondria specific autophagy (mitophagy), we also assessed the steady-state levels of mitochondrial markers to determine whether DJ-1 may also play a role. As shown in Figure 8E, loss of DJ-1 does not induce significantly altering the expression of *cytochrome c* oxidase (COX) subunits of complex I or complex V. Furthermore, expression of the outer mitochondrial membrane marker Tom20 was also unchanged. This suggests that mitophagy, at least at a gross level, is not affected by the loss of DJ-1. This theory is supported by initial observations that Parkin is not significantly recruited to mitochondria in DJ-1 KO cells under basal conditions (Joselin *et al.*, unpublished data).

Mitochondrial morphology and autophagy are also perturbed in human DJ-1-linked Parkinson's disease

Finally, to provide evidence that the DJ-1-dependent perturbations in mitochondrial homeostasis also extend to a human model of DJ-1-linked PD, we obtained human lymphoblasts isolated from control and PD patients. The PD lymphoblasts were obtained from an Italian and Dutch family, respectively (12). The previously described L166P pathogenic mutation found in the Italian family consists of a leucine to proline substitution at amino acid 166, while the Deletion (Del) mutation, found in a Dutch family, results from a complete loss of exons 1–5 (12). As shown in Figure 9A, similar to the pattern of

mitochondrial morphology observed in DJ-1^{+/+} and DJ-1^{-/-} murine tissues, electron microscopic analysis of lymphoblasts isolated from human PD patients (L166P, DEL) contained a greater percentage of fragmented mitochondria compared with control lymphoblasts (i.e. $< 0.5 \mu\text{m}$; $41.578 \pm 2.41\%$ and $48.316 \pm 6.02\%$ in PD versus $12.62 \pm 3.03\%$ and $9.755 \pm 2.23\%$ in controls) and a smaller percentage of mitochondria that were longer than $> 1.0 \mu\text{m}$ ($23.019 \pm 0.84\%$ and $23.997 \pm 0.94\%$ in PD versus $41.578 \pm 2.41\%$ and $48.316 \pm 6.02\%$ in controls; Fig. 9B). We also evaluated whether autophagy was similarly affected in human DJ-1-linked PD and observed that p62 was decreased in both PD patient cell lines when compared with CTRL lymphoblasts (Fig. 9C). These data confirm that the mitochondrial morphology as well as changes in autophagic markers observed in DJ-1^{+/+} and DJ-1^{-/-} are also present in human DJ-1-linked PD.

DISCUSSION

Mitochondrial dysfunction appears to contribute to the progression of sporadic PD and it has been postulated that excess ROS produced as the result of mitochondrial dysfunction may be an important reason for which neurons exhibit increased sensitivity to oxidative stress-induced neuronal cell death (36,37). Emerging evidence points to underlying defects in mitochondrial morphology and dynamics as a potential mechanism to explain this increased sensitivity (38). In PD, this relationship is significant since several PD-linked genes (DJ-1, Parkin, Pink1) have been found to reside or translocate to the mitochondrial compartments (7,8,29,39–42), participate in mitochondrial remodeling (7,9–11) and actively regulate mitochondrial quality control (18,19,41–43). Of the three PD-linked genes that have been associated with mitochondria, the least is known regarding the role of DJ-1.

Mitochondrial morphology, dynamics and ROS production are altered by the loss of DJ-1

We first began our investigation by characterizing the impact of DJ-1 deficiency on mitochondrial morphology and function under steady-state conditions in a variety of experimental systems. We demonstrated both *in vitro* and *in vivo* neuronal and non-neuronal cells, as well as in brain tissue that mitochondria are significantly more fragmented with the loss of DJ-1. Importantly, we also extended these findings to human DJ-1-linked PD to convincingly implicate that an aberrant DJ-1-dependent mitochondrial phenotype in a more disease relevant model. We also demonstrated that the mitochondrial phenotype produced by the loss of DJ-1 contributes to the

antibodies to Tom20 (red) to visualize mitochondria. Inset: lower magnification images. (D) Quantification of mitochondrial lengths as described previously [Jahani-Asl *et al.* (20); $n = 3$ independent experiments with a minimum of 500 mitochondria/experiment that were counted per condition]. Scale bar = $5 \mu\text{m}$. * $P < 0.05$ versus respective controls. (E) Confocal images from SH-5Y5Y cells in which DJ-1 has been knocked down via siRNA, and transfected with DJ-1, Parkin or PINK1 as described in the Materials and Methods. Inset: lower magnification images. (F) Quantification of at least 300 cells/condition was performed as described in the Materials and Methods. Data are representative of at least three independent experiments where each condition was done in triplicate. OE, overexpression. Scale bar = $5 \mu\text{m}$. * $P < 0.05$ versus siDJ-1- and # $P < 0.05$ versus siDJ-1.

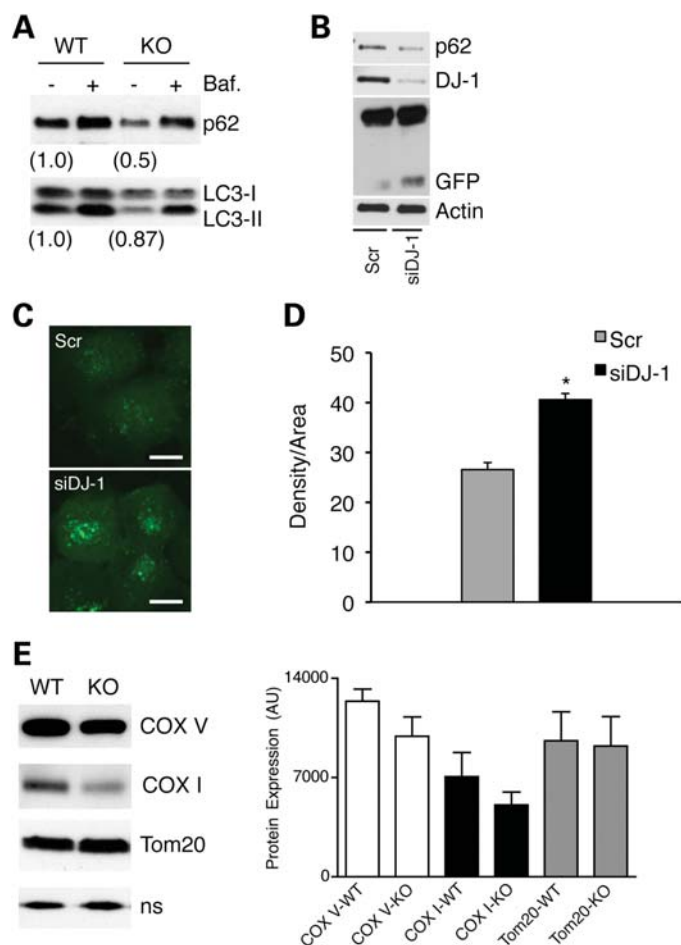


Figure 8. Cells deficient for DJ-1 undergo enhanced autophagic activity. (A) Proteins were extracted from WT and KO DJ-1 MEFs treated with (+) or without (–) Bafilomycin (10 μ g/ml, 3 h) and subjected to western blotting for p62 and LC3-I and LC3-II levels. Numbers below representative images refer to fold changes versus WT (-Baf) after correction for actin. Data are representative of three independent experiments. (B) Total cell lysates from H1299 cells stably expressing GFP-LC3 and transfected with either scrambled (Scr) or a siRNA against DJ-1 (siDJ-1) were analyzed by western blotting for DJ-1, p62 and free GFP. Data are representative of at least three independent experiments. (C) Confocal images of H1299 cells stably expressing GFP-LC3 cells transfected with either scrambled (Scr) or a siRNA against DJ-1 (siDJ-1). (D) The density of GFP puncta in Scr versus siDJ-1 conditions was analyzed in at least 150 cells/condition. Data are representative of three independent experiments * P < 0.05, siDJ-1 versus Scr. control. Scale bar = 2 μ m. (E) Total cell lysates from DJ-1 WT and KO MEFs were subjected to western blotting for COX V, COX I and Tom20 levels (n.s., non-specific band was used as a loading control). Data are representative of five to seven independent experiments.

oxidative stress-induced sensitivity to cell death since reversal of the mitochondrial phenotype by overexpression of DN-Drp1 to rescue mitochondrial fragmentation abrogated neuronal cell death induced by MPP+. Is the fragmented phenotype a result of increased fission or decreased fusion? Since mitochondrial fusion rates and the steady state levels of the mitochondrial fusion protein MFN1 are decreased in DJ-1 deficient cells, we would be tempted to speculate that mitochondrial fusion is decreased. However, our results also do not rule out that an increase in mitochon-

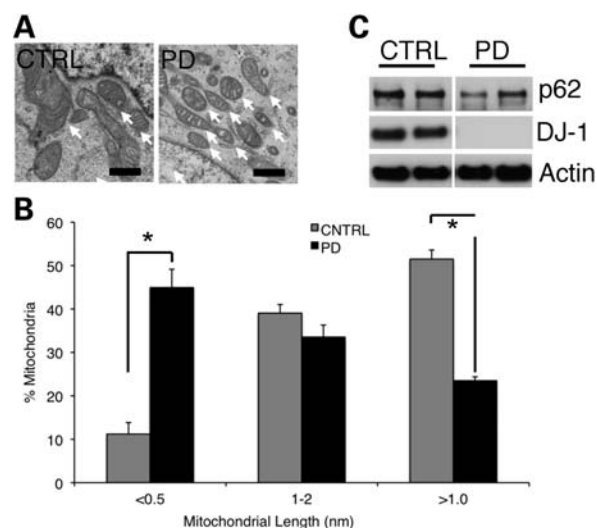


Figure 9. Mitochondrial morphology and autophagy are also perturbed in human DJ-1-linked PD. (A) EM images of mitochondria from human lymphoblasts isolated from healthy control (C48 and GEPA) and PD (L166P and Del) patients. (B) Quantification of mitochondrial diameters in human lymphoblasts (n = 4; at least 200 mitochondria/experiment were counted). Scale bar = 500 nm. * P < 0.05, PD versus control. (C) Total protein was extracted from human control (CTRL), and PD (L166P and Del) lymphoblasts were subjected to western blotting for DJ-1, p62 and actin. Data are quantified as the relative changes in steady state protein levels corrected for loading using actin. Five independent experiments are represented. * P < 0.05, PD versus control. White arrows in (A) depict mitochondria.

drial fission is also a possibility. Indeed, during the preparation of this manuscript, Krebiehl *et al.* (44) demonstrated that altered mitochondrial morphology induced by the loss of DJ-1 could be attributed to changes in mitochondrial fusion or fission that occurs with DJ-1 deficiency could readily explain the increased sensitivity of these cells to oxidative stress (14), as it is known that fragmented mitochondria precedes apoptosis, or alternatively renders mitochondria more susceptible to death-inducing stimuli (20,45–48).

ROS is important in establishing the DJ-1-dependent phenotype

Based on the known impact of excess ROS on mitochondrial morphology (23), we suspected that the increased ROS produced by mitochondria from DJ-1^{-/-} animals could be responsible for the fragmented phenotype. Indeed, we confirmed this hypothesis by first demonstrating that scavenging ROS with the use of NAC or WT DJ-1 (itself a suspected free radical scavenger), but not an oxidant mutant of DJ-1 (C106A), was able to rescue the fragmented phenotype observed in DJ-1 deficient primary cortical neurons. Our data also show that while the excess H₂O₂ produced within mitochondria by the loss of DJ-1 is sufficient to alter mitochondrial morphology, they are not produced in sufficient concentrations to cause overt changes in mitochondrial oxygen consumption and citrate synthase activity, at least in the

brain. In all likelihood, these factors contribute to the lack of any gross neuronal abnormalities including dopaminergic neuron numbers in the substantia nigra, fiber densities and dopamine levels in the striatum and the absence of any behavioral deficits in untreated DJ-1 deficient mice (14). It is therefore more likely that DJ-1 deficiency compromises the sub-cellular milieu rendering them more vulnerable to additional stress. Indeed, the observation that DJ-1 deficiency does not seem to grossly affect mitophagy leading to the accumulation, instead of the removal of fragmented mitochondria further adds to this possibility. This theory is also supported by initial observations that Parkin is not significantly recruited to mitochondria in DJ-1 KO cells under basal conditions (Joselin *et al.*, unpublished data).

Indeed, as we have previously demonstrated, DJ-1 deficient animals/cells are hypersensitive to MPTP or hydrogen peroxide treatment and this hypersensitization results in the previously described dopaminergic cell death and behavioral deficits, effectively recapitulating some pathological and clinical features of human PD (14).

Pink1 and Parkin can rescue DJ-1 deficient mitochondrial fragmentation

We also assessed the relationship of DJ-1 with Parkin and Pink1, two recessively linked PD genes, as they have all been implicated in regulating aspects of mitochondrial morphology and/or dynamics. Previous studies using the *Drosophila melanogaster* model have shown that the loss of Pink1 and Parkin independently compromise mitochondrial integrity (9,11,28,49). Since double mutants produce an identical phenotype to each mutant alone, and overexpression of Parkin rescues Pink1 deficits but not *vice versa*, it was postulated that they function in the same pathway with Pink1 positioned upstream of Parkin (9,11,28,49). More recently, it has been shown that Pink1 and Parkin actively participate in mitochondrial quality control (18,19,41–43). Given that DJ-1 deficiency induces oxidative stress and mitochondrial defects, we hypothesized that overexpression of these mitochondrial quality control factors would rescue the DJ-1 deficient mitochondrial phenotype. We confirmed this hypothesis using two different models. First, Pink1 and Parkin were overexpressed in DJ-1 deficient primary cortical neurons. In this model, overexpression of either Pink1 or Parkin rescued the fragmented mitochondrial phenotype in DJ-1 deficient cells. Second, we used a dopaminergic cell line to overexpress Pink1 and Parkin in cells where DJ-1 levels were reduced down by siRNA. Similar to our findings in primary cortical neurons, the DJ-1-induced fragmentation phenotype produced by knockdown of DJ-1 was reversed with overexpression of either Pink1 or Parkin. It is important to stress that the exact mechanistic link between DJ-1 and Pink/Parkin is not clear. However, we would propose that DJ-1 somehow modulates the actions or activity of Pink1 and/or Parkin, possibly via its effect on the ROS environment. Given the effects of Parkin and PINK1 deficiency on antioxidant capacity and ROS production (50–52), it is also tempting to speculate that overexpression of either gene could potentially ameliorate that ROS milieu of the DJ-1 deficient cells, thereby reversing

the fragmented phenotype. Alternatively, a more direct regulation is also possible.

DJ-1 deficiency increases autophagic activity

Increasing evidence has implicated several PD-linked genes including Pink and Parkin in the process of autophagy (18,19,41–43). Two recently published studies have now implicated DJ-1 (19,44). We also pursued this phenomenon in the present manuscript and suggest that the loss of DJ-1 promotes enhanced autophagy resulting in increased turnover. According to Mizushima and Yoshimori (34) and Rubinsztein *et al.* (35), a loss in the levels of the autophagy markers LC3-II and p62 at a given time is either attributed to a downregulation of autophagosome formation or enhanced degradation. If the level of LC3-II or p62 rises following incubation with autophagy inhibitors such as Bafilomycin A1, as was seen in the present study, it is considered that during the course of the experimental time frame that the number of molecules degraded exceeds the number being produced. We further assessed the effect of transient DJ-1 knockdown on autophagic activity and found that within 48 h of DJ-1 knockdown, the autophagy was increased, as measured by the decrease in p62 levels and the increase in LC3 puncta formation. It has previously been shown that following acute starvation, autophagy is increased and that prolonged starvation leads to excessive activity and turnover (35). Acute starvation led to decreased p62 levels and LC3 puncta formation, whereas a complete loss of LC3-II levels was observed during prolonged starvation. By analogy, one could interpret that acute DJ-1 knockdown results increase autophagic activity, while germline deletion is associated with excessive autophagic activity resulting in increased turnover. In either condition, autophagic activity is enhanced with DJ-1 deficiency. Future studies will more carefully evaluate the nature of this phenomenon. Additionally, whether DJ-1 more directly regulates the autophagic response or merely influences the ROS environment leading to increased flux is unknown and warrants further study. The evidence suggesting that ROS triggers autophagy would be in keeping with the latter suggestion (53–55). Furthermore, the idea that DJ-1 participates in the Pink1/Parkin pathway tentatively suggests the possibility that DJ-1 could modulate Pink1/Parkin activity and thereby regulate autophagic activity. Alternatively, DJ-1 may more directly regulate additional upstream activators of autophagy, including mTOR and AMPK, which has been suggested previously (19). More careful analyses will be required to validate these possibilities.

In conclusion, this study demonstrates that DJ-1 plays an active role in the remodeling of mitochondria and regulation of autophagy. Cells lacking DJ-1 display a fragmented mitochondrial morphology that can be rescued with ROS scavengers, wild-type DJ-1, Parkin and Pink1. This DJ-1-dependent mitochondrial morphology contributes to oxidative stress-induced sensitivity to cell death since reversal of this mitochondrial phenotype abrogates neuronal cell death. Finally, we also show that DJ deficiency leads to altered autophagy in DJ-1-deficient murine and human cells. We propose that under conditions of oxidative stress, these derangements may account for the reported increased sensitivity to cell death of DJ-1 deficient neurons.

MATERIALS AND METHODS

Antibodies

The following antibodies were used in this study: mouse anti-Drp-1 (BD Transduction), chicken anti-MFN1 (Novus Biological), rabbit anti-MFN2 (Santa Cruz), mouse anti-COX V (Mitosciences), mouse anti-COX I (Mitosciences), rabbit anti-Tom20 (Santa Cruz), rabbit anti-LC3 (Novus Biologicals), guinea pig anti-p62 (ARP), mouse anti-p62 (Santa Cruz), mouse anti DJ-1 (Stressgen), mouse anti-parkin mouse PRK8 (Santa Cruz), anti-PINK1 polyclonal antibody (Novus Biologicals), anti-DJ1 polyclonal antibody (Abcam), mouse anti- β -actin (Sigma), horseradish peroxidase-conjugated secondary antibodies (Bio-Rad).

Cell lines, transfections, viral infections and plasmids

MEFs and primary cortical neurons were derived from E14.5–15.5 transgenic DJ-1 animals as previously described (14). Immortalized human lymphoblasts obtained from DJ-1-linked PD (Del or L166P) or healthy controls were cultured as described previously (56). H1299 cell line stably expressing GFP-LC3 cultured as previously described (57). SH-5Y5Y cells were cultivated as previously described (58). For RNA interference, SH-5Y5Y or H1299 cells were reverse-transfected with Stealth siRNA (Invitrogen) using Lipofectamine RNAiMAX (Invitrogen) or siRNA (Santa Cruz) using siLentFect (Bio-Rad), respectively, according to the manufacturer's instructions. *DNA Constructs (SH-5Y5Y cells)*: Human wild-type (wt) parkin and human wild-type PINK1 were described earlier (49,59). Human wild-type DJ was amplified from a human brain cDNA library and inserted into the pcDNA3.1 vector (Invitrogen). *Viral plasmids and infections (primary cortical neurons)*: for rescue studies, cortical neurons were harvested from DJ-1^{+/+} or DJ-1^{-/-} littermate embryos (produced by a heterozygote cross) at E15.5 and plated at a density of 150 000 cells per well (24-well dish) on glass cover slips coated with 1XPoly-D-Lysine. Viral particles expressing GFP, DJ-1, DJ-1 C106A, Pink1 or Parkin were administered at a multiplicity of infection (MOI) of 30 at the time of plating. Cortical neurons infected with DJ-1, DJ-1C106A and Pink1 were harvested 48 h following infection. Cortical neurons infected with Parkin were harvested 4 days post-infection and plating. For cell survival studies, cortical neurons harvested as described above were infected with either control (EGFP) adenovirus or dominant-negative Drp-1 (ECFP-C1 DLVP K38E) adenoviruses at MOI of 40 and then immediately seeded into 24-well plates at an approximate density of 350 000 neurons/well. Neurons were cultured for 3 days and then treated with 10 μ M MPP⁺ for 24 h.

Cell survival

Neuronal survival was evaluated by assessing nuclear integrity of GFP/CFP-positive neurons as done previously (14).

Citrate synthase activity

Maximal activity of citrate synthase (EC 4.1.3.7) was measured at 25°C in previously frozen homogenate and mitochondria from brain and skeletal as previously described (60).

Confocal microscopy/immunofluorescence/mitochondrial fusion rates

Confocal images were acquired with a 63 \times objective (1.4) by an inverted Laser Scanning Microscope (LSM510 META, Zeiss). Mitochondrial fusion rates were calculated as previously described (21).

Generation and genotyping of DJ-1 mice

The generation and genotype of the DJ-1 deficient mice has previously been described in detail (61).

H₂O₂ generation

Mitochondrial H₂O₂ production rate was determined in freshly isolated mitochondria from skeletal muscle and brain using the *p*-hydroxyphenylacetate (PHPA) fluorometric assay (62). Mitochondria (0.1 mg/ml) were incubated in standard incubation medium (IM: 120 mM KCl, 1 mM EGTA, 5 mM KH₂PO₄, 2 mM MgCl₂ and 3 mM HEPES; pH 7.4) supplemented with 0.3% defatted BSA. H₂O₂ production was monitored for up to 25 min using a temperature-controlled fluorimeter (BioTek, FLx800) at 37°C. Fluorescence readings were converted to H₂O₂ production rates by use of a standard curve.

Immunofluorescence (primary cortical neurons and MEFs)

Cortical neurons or MEFs were fixed with 4% PFA diluted in cell culture medium for 15 min at 37°C. Cells were then washed 3 \times with 1XPBS. Immediately following this, cells were permeabilized and blocked with 10% normal goat serum-0.1% Triton X/PBS for 1 h at room temperature. Cells were then stained with Tom-20 (1:100, a kind gift from Dr Gordon Shore or from Santa Cruz) or *cytochrome c* (1:100, BD Biosciences, in 5% normal goat serum overnight at 4°C) for the visualization of mitochondria. The following day, cells were washed 3 \times with 5% normal goat serum/PBS and then incubated for 1 h with the appropriate Alexa conjugated fluorophores in 5% normal goat serum/PBS. Cells were then washed 3 \times with 1XPBS, rinsed in sterile H₂O and mounted onto microscope slides using Gel Mount (Sigma).

Fluorescent staining of mitochondria and western blot analysis (SH-5Y5Y cells)

SH-5Y5Y cells were grown on 15 mm glass cover slips. Cells were fluorescently labeled with 0.1 μ M DiOC₆ (3) in cell culture medium for 15 min. After washing the cover slips with medium, living cells were analyzed for mitochondrial morphology by fluorescence microscopy using a Leica DMRB microscope (Leica, Wetzlar, Germany). Cells were categorized in two classes according to their mitochondrial morphology: tubular or fragmented. Cells displaying an intact network of tubular mitochondria were classified as tubular. When this network was disrupted and mitochondria appeared predominantly spherical or rod-like, they were classified as fragmented. The mitochondrial morphology of at least 300 cells per plate was determined in a blinded manner, i.e. the researcher was blind to the transfection status.

Quantifications were based on triplicates of at least three independent experiments. Proteins were analyzed by SDS–PAGE and western blotting using polyvinylidene difluoride membranes (Millipore, Schwalbach, Germany). The membranes were blocked with 5% non-fat dry milk in TBS containing 0.1% Tween 20 (TBS-T) for 1 h at room temperature and then incubated with the primary antibody in blocking solution for 16 h at 4°C. After extensive washing with TBS-T, the membranes were incubated with HRP-conjugated secondary antibody for 60 min at room temperature. Following washing with TBS-T, the antigen was detected with the enhanced chemiluminescence (ECL) detection system or ECL plus detection system (Amersham Biosciences, Freiburg, Germany).

Immunoblotting

Cell lysis was carried out identically for both MEFs and neurons. Cells were washed twice with PBS, scraped in lysis buffer containing 50 mM Tris–HCl pH 7.5, 100 mM NaCl, 0.4% Triton X-100, 1 mM DTT and 1× protease inhibitor cocktail (Roche). Samples were kept on ice for 20 min and then spun with maximal speed at 20 000g at 4°C for 5 min. Protein quantification was carried out using both Bradford (Bio-Rad) and BCA (Pierce) methods. Fifteen micrograms of each lysate was electrophoresed on 12% SDS–polyacrylamide gels, or 4–20% gradient gels (Invitrogen) and transferred to polyvinylidene fluoride (PVDF) or nitrocellulose membranes (Millipore). For tissue lysates, 15 µg of each tissue lysate was electrophoresed on 12% SDS–PAGE gels and transferred to polyvinylidene fluoride (PVDF) or nitrocellulose membranes (Millipore).

Isolation of mitochondria

DJ-1^{+/+} or DJ-1^{-/-} mice (4–6 months old) were euthanized by decapitation for isolation of skeletal muscle and brain mitochondria. Isolation of skeletal muscle mitochondria was performed using a modified method of Chappell and Perry (63), as previously described in detail (64). Brain mitochondria were isolated as described (50).

Lentivirus production and transduction

Lentiviral vectors were generated by transient transfection in 293T cells using PEI. The constructs for manufacturing the lentiviruses were obtained from Addgene.org. Protocols used to manufacture and purify lentiviruses were done according to Tronolab's protocols (www.tronolab.com).

Oxygen consumption

Oxygen consumption was measured in isolated brain mitochondria (0.3 mg/ml) at 37°C using a Clark-type oxygen electrode (Hansatech, Norfolk, UK), incubated in standard incubation medium (IM: 120 mM KCl, 1 mM EGTA, 5 mM KH₂PO₄, 2 mM MgCl₂ and 3 mM HEPES; pH 7.4) containing 0.3% defatted BSA and assumed to contain 406 nmol O/ml at 37°C (65). State 3 (maximum phosphorylating) respiration was determined using 5 mM glutamate/5 mM malate as substrate, and 500 µM ADP. State 4 (non-phosphorylating or

maximal leak-dependent respiration) was determined following addition of oligomycin (8 µg/ml). All measurements were performed in duplicate.

Statistical analyses

Unless otherwise described, data analysis was carried out using independent two-tailed *t*-tests. Significance was marked by * when *P* < 0.05. All data are presented as means ± SEM.

SUPPLEMENTARY MATERIAL

Supplementary Material is available at *HMG* online.

ACKNOWLEDGEMENTS

The authors would like to thank Dr Gordon Shore (McGill University, Montreal, Canada) for the provision of the GFP-LC3 stable cell line and the α-Tom20 antibody. The authors also wish to thank Paul Marcogliese and Viola Mugamba for technical assistance, and Dr Marc Germain for helpful insights on the manuscript.

Conflict of Interest statement. None declared.

FUNDING

This work was supported by grants from the Canadian Institutes of Health Research (CIHR), Heart and Stroke Foundation of Ontario (HSFO), Neuroscience Canada (Brain Repair Grant), Parkinson's Society Canada (PSC), Parkinson's Disease Foundation (PDF) and World Class University program through the National Research Foundation of Korea funded by the Ministry of Education, Science and Technology, South Korea (R31-2008-000-20004-0) to D.S.P. I.I. was supported by a CIHR Postdoctoral fellowship. H.A. was supported by a Heart and Stroke Foundation of Canada doctoral award. E.L.S. was supported by a Canadian Diabetes Association (CDA) Postdoctoral fellowship. A.J.-A. was supported by a CIHR doctoral award. M.W.C.R. was supported by a Heart and Stroke Foundation of Ontario Master's student award; S.C. was supported by a summer student award from the centre for stroke recovery (CSR); S.J.H. was supported by PSC Master's Student award.

REFERENCES

1. Abou-Sleiman, P.M., Muqit, M.M. and Wood, N.W. (2006) Expanding insights of mitochondrial dysfunction in Parkinson's disease. *Nat. Rev.*, **7**, 207–219.
2. Schapira, A.H. (1998) Mitochondrial dysfunction in neurodegenerative disorders. *Biochim. Biophys. Acta*, **1366**, 225–233.
3. Mann, V.M., Cooper, J.M., Krige, D., Daniel, S.E., Schapira, A.H. and Marsden, C.D. (1992) Brain, skeletal muscle and platelet homogenate mitochondrial function in Parkinson's disease. *Brain*, **115**, 333–342.
4. Bindoff, L.A., Birch-Machin, M.A., Carlidge, N.E., Parker, W.D. Jr and Turnbull, D.M. (1991) Respiratory chain abnormalities in skeletal muscle from patients with Parkinson's disease. *J. Neurol. Sci.*, **104**, 203–208.

5. Drechsel, D.A. and Patel, M. (2008) Role of reactive oxygen species in the neurotoxicity of environmental agents implicated in Parkinson's disease. *Free Radic. Biol. Med.*, **44**, 1873–1886.
6. Cleeter, M.W., Cooper, J.M. and Schapira, A.H. (1992) Irreversible inhibition of mitochondrial complex I by 1-methyl-4-phenylpyridinium: evidence for free radical involvement. *J. Neurochem.*, **58**, 786–789.
7. Silvestri, L., Caputo, V., Bellacchio, E., Atorino, L., Dallapiccola, B., Valente, E.M. and Casari, G. (2005) Mitochondrial import and enzymatic activity of PINK1 mutants associated to recessive parkinsonism. *Hum. Mol. Genet.*, **14**, 3477–3492.
8. Zhou, C., Huang, Y., Shao, Y., May, J., Prou, D., Perier, C., Dauer, W., Schon, E.A. and Przedborski, S. (2008) The kinase domain of mitochondrial PINK1 faces the cytoplasm. *Proc. Natl Acad. Sci. USA*, **105**, 12022–12027.
9. Poole, A.C., Thomas, R.E., Andrews, L.A., McBride, H.M., Whitworth, A.J. and Pallanck, L.J. (2008) The PINK1/Parkin pathway regulates mitochondrial morphology. *Proc. Natl Acad. Sci. USA*, **105**, 1638–1643.
10. Deng, H., Dodson, M.W., Huang, H. and Guo, M. (2008) The Parkinson's disease genes pink1 and parkin promote mitochondrial fission and/or inhibit fusion in *Drosophila*. *Proc. Natl Acad. Sci. USA*, **105**, 14503–14508.
11. Clark, I.E., Dodson, M.W., Jiang, C., Cao, J.H., Huh, J.R., Seol, J.H., Yoo, S.J., Hay, B.A. and Guo, M. (2006) *Drosophila* pink1 is required for mitochondrial function and interacts genetically with parkin. *Nature*, **441**, 1162–1166.
12. Bonifati, V., Rizzu, P., van Baren, M.J., Schaap, O., Breedveld, G.J., Krieger, E., Dekker, M.C., Squitieri, F., Ibanez, P., Joesse, M. *et al.* (2003) Mutations in the DJ-1 gene associated with autosomal recessive early-onset parkinsonism. *Science*, **299**, 256–259.
13. Aleyasin, H., Rousseaux, M.W., Phillips, M., Kim, R.H., Bland, R.J., Callaghan, S., Slack, R.S., During, M.J., Mak, T.W. and Park, D.S. (2007) The Parkinson's disease gene DJ-1 is also a key regulator of stroke-induced damage. *Proc. Natl Acad. Sci. USA*, **104**, 18748–18753.
14. Kim, R.H., Smith, P.D., Aleyasin, H., Hayley, S., Mount, M.P., Pownall, S., Wakeham, A., You-Ten, A.J., Kalia, S.K., Horne, P. *et al.* (2005) Hypersensitivity of DJ-1-deficient mice to 1-methyl-4-phenyl-1,2,3,6-tetrahydropyridine (MPTP) and oxidative stress. *Proc. Natl Acad. Sci. USA*, **102**, 5215–5220.
15. Andres-Mateos, E., Perier, C., Zhang, L., Blanchard-Fillion, B., Greco, T.M., Thomas, B., Ko, H.S., Sasaki, M., Ischiropoulos, H., Przedborski, S. *et al.* (2007) DJ-1 gene deletion reveals that DJ-1 is an atypical peroxiredoxin-like peroxidase. *Proc. Natl Acad. Sci. USA*, **104**, 14807–14812.
16. Taira, T., Saito, Y., Niki, T., Iguchi-Ariga, S.M., Takahashi, K. and Ariga, H. (2004) DJ-1 has a role in antioxidative stress to prevent cell death. *EMBO Rep.*, **5**, 213–218.
17. Park, J., Kim, S.Y., Cha, G.H., Lee, S.B., Kim, S. and Chung, J. (2005) *Drosophila* DJ-1 mutants show oxidative stress-sensitive locomotive dysfunction. *Gene*, **361**, 133–139.
18. Gonzalez-Polo, R., Niso-Santano, M., Moran, J.M., Ortiz-Ortiz, M.A., Bravo-San Pedro, J.M., Soler, G. and Fuentes, J.M. (2009) Silencing DJ-1 reveals its contribution in paraquat-induced autophagy. *J. Neurochem.*, **109**, 889–898.
19. Vasseur, S., Afzal, S., Tardivel-Lacombe, J., Park, D.S., Iovanna, J.L. and Mak, T.W. (2009) DJ-1/PARK7 is an important mediator of hypoxia-induced cellular responses. *Proc. Natl Acad. Sci. USA*, **106**, 1111–1116.
20. Jahani-Asl, A., Cheung, E.C., Neuspiel, M., MacLaurin, J.G., Fortin, A., Park, D.S., McBride, H.M. and Slack, R.S. (2007) Mitofusin 2 protects cerebellar granule neurons against injury-induced cell death. *J. Biol. Chem.*, **282**, 23788–23798.
21. Zunino, R., Schauss, A., Rippstein, P., Andrade-Navarro, M. and McBride, H.M. (2007) The SUMO protease SENP5 is required to maintain mitochondrial morphology and function. *J. Cell Sci.*, **120**, 1178–1188.
22. Kopin, I.J. and Markey, S.P. (1988) MPTP toxicity: implications for research in Parkinson's disease. *Annu. Rev. Neurosci.*, **11**, 81–96.
23. Barsoum, M.J., Yuan, H., Gerencser, A.A., Liot, G., Kushnareva, Y., Graber, S., Kovacs, I., Lee, W.D., Waggoner, J., Cui, J. *et al.* (2006) Nitric oxide-induced mitochondrial fission is regulated by dynamin-related GTPases in neurons. *EMBO J.*, **25**, 3900–3911.
24. Mitumoto, A., Nakagawa, Y., Takeuchi, A., Okawa, K., Iwamatsu, A. and Takanezawa, Y. (2001) Oxidized forms of peroxiredoxins and DJ-1 on two-dimensional gels increased in response to sublethal levels of paraquat. *Free Radic. Res.*, **35**, 301–310.
25. Canet-Aviles, R.M., Wilson, M.A., Miller, D.W., Ahmad, R., McLendon, C., Bandyopadhyay, S., Baptista, M.J., Ringe, D., Petsko, G.A. and Cookson, M.R. (2004) The Parkinson's disease protein DJ-1 is neuroprotective due to cysteine-sulfenic acid-driven mitochondrial localization. *Proc. Natl Acad. Sci. USA*, **101**, 9103–9108.
26. Meulener, M.C., Xu, K., Thomson, L., Ischiropoulos, H. and Bonini, N.M. (2006) Mutational analysis of DJ-1 in *Drosophila* implicates functional inactivation by oxidative damage and aging. *Proc. Natl Acad. Sci. USA*, **103**, 12517–12522.
27. Whitworth, A.J. and Pallanck, L.J. (2009) The PINK1/Parkin pathway: a mitochondrial quality control system? *J. Bioenerg. Biomembr.*, **41**, 499–503.
28. Park, J., Lee, G. and Chung, J. (2009) The PINK1-Parkin pathway is involved in the regulation of mitochondrial remodeling process. *Biochem. Biophys. Res. Commun.*, **378**, 518–523.
29. Vives-Bauza, C., Zhou, C., Huang, Y., Cui, M., de Vries, R.L., Kim, J., May, J., Tocilescu, M.A., Liu, W., Ko, H.S. *et al.* (2010) PINK1-dependent recruitment of Parkin to mitochondria in mitophagy. *Proc. Natl Acad. Sci. USA*, **107**, 378–383.
30. Geisler, S., Holmstrom, K.M., Skujat, D., Fiesel, F.C., Rothfuss, O.C., Kahle, P.J. and Springer, W. (2010) PINK1/Parkin-mediated mitophagy is dependent on VDAC1 and p62/SQSTM1. *Nat. Cell Biol.*, **12**, 119–131.
31. Narendra, D.P., Jin, S.M., Tanaka, A., Suen, D.F., Gautier, C.A., Shen, J., Cookson, M.R. and Youle, R.J. (2010) PINK1 is selectively stabilized on impaired mitochondria to activate parkin. *PLoS Biol.*, **8**, e1000298.
32. Haque, M.E., Thomas, K.J., D'Souza, C., Callaghan, S., Kitada, T., Slack, R.S., Fraser, P., Cookson, M.R., Tandon, A. and Park, D.S. (2008) Cytoplasmic Pink1 activity protects neurons from dopaminergic neurotoxin MPTP. *Proc. Natl Acad. Sci. USA*, **105**, 1716–1721.
33. Klionsky, D.J., Abeliovich, H., Agostinis, P., Agrawal, D.K., Aliev, G., Askew, D.S., Baba, M., Baehrecke, E.H., Bahr, B.A., Ballabio, A. *et al.* (2008) Guidelines for the use and interpretation of assays for monitoring autophagy in higher eukaryotes. *Autophagy*, **4**, 151–175.
34. Mizushima, N. and Yoshimori, T. (2007) How to interpret LC3 immunoblotting. *Autophagy*, **3**, 542–545.
35. Rubinsztein, D.C., Cuervo, A.M., Ravikumar, B., Sarkar, S., Korolchuk, V., Kaushik, S. and Klionsky, D.J. (2009) In search of an 'autophagometer'. *Autophagy*, **5**, 585–589.
36. Giasson, B.I., Ischiropoulos, H., Lee, V.M. and Trojanowski, J.Q. (2002) The relationship between oxidative/nitrative stress and pathological inclusions in Alzheimer's and Parkinson's diseases. *Free Radic. Biol. Med.*, **32**, 1264–1275.
37. Perkins, G., Bossy-Wetzel, E. and Ellisman, M.H. (2009) New insights into mitochondrial structure during cell death. *Exp. Neurol.*, **218**, 183–192.
38. Knott, A.B., Perkins, G., Schwarzenbacher, R. and Bossy-Wetzel, E. (2008) Mitochondrial fragmentation in neurodegeneration. *Nat. Rev.*, **9**, 505–518.
39. Lev, N., Ickowicz, D., Melamed, E. and Offen, D. (2008) Oxidative insults induce DJ-1 upregulation and redistribution: implications for neuroprotection. *Neurotoxicology*, **29**, 397–405.
40. Junn, E., Jang, W.H., Zhao, X., Jeong, B.S. and Mouradian, M.M. (2009) Mitochondrial localization of DJ-1 leads to enhanced neuroprotection. *J. Neurosci. Res.*, **87**, 123–129.
41. Narendra, D., Tanaka, A., Suen, D.F. and Youle, R.J. (2009) Parkin-induced mitophagy in the pathogenesis of Parkinson disease. *Autophagy*, **5**, 706–708.
42. Narendra, D., Tanaka, A., Suen, D.F. and Youle, R.J. (2008) Parkin is recruited selectively to impaired mitochondria and promotes their autophagy. *J. Cell Biol.*, **183**, 795–803.
43. Cherra, S.J. 3rd, Dagda, R.K., Tandon, A. and Chu, C.T. (2009) Mitochondrial autophagy as a compensatory response to PINK1 deficiency. *Autophagy*, **5**, 1213–1214.
44. Krebiel, G., Ruckerbauer, S., Burbulla, L.F., Kieper, N., Maurer, B., Waak, J., Wolburg, H., Gizatullina, Z., Gellerich, F.N., Voitalla, D. *et al.* (2010) Reduced basal autophagy and impaired mitochondrial dynamics due to loss of Parkinson's disease-associated protein DJ-1. *PLoS ONE*, **5**, e9367.
45. Delivani, P., Adrain, C., Taylor, R.C., Duriez, P.J. and Martin, S.J. (2006) Role for CED-9 and Egl-1 as regulators of mitochondrial fission and fusion dynamics. *Mol. Cell*, **21**, 761–773.
46. Frank, S., Gaume, B., Bergmann-Leitner, E.S., Leitner, W.W., Robert, E.G., Catez, F., Smith, C.L. and Youle, R.J. (2001) The role of dynamin-related

- protein 1, a mediator of mitochondrial fission, in apoptosis. *Dev. Cell*, **1**, 515–525.
47. Karbowski, M., Amoult, D., Chen, H., Chan, D.C., Smith, C.L. and Youle, R.J. (2004) Quantitation of mitochondrial dynamics by photolabeling of individual organelles shows that mitochondrial fusion is blocked during the Bax activation phase of apoptosis. *J. Cell Biol.*, **164**, 493–499.
 48. Lee, Y.J., Jeong, S.Y., Karbowski, M., Smith, C.L. and Youle, R.J. (2004) Roles of the mammalian mitochondrial fission and fusion mediators Fis1, Drp1 and Opa1 in apoptosis. *Mol. Biol. Cell*, **15**, 5001–5011.
 49. Exner, N., Treske, B., Paquet, D., Holmstrom, K., Schiesling, C., Gispert, S., Carballo-Carbajal, I., Berg, D., Hoepken, H.H., Gasser, T. *et al.* (2007) Loss-of-function of human PINK1 results in mitochondrial pathology and can be rescued by parkin. *J. Neurosci.*, **27**, 12413–12418.
 50. Palacino, J.J., Sagi, D., Goldberg, M.S., Krauss, S., Motz, C., Wacker, M., Klose, J. and Shen, J. (2004) Mitochondrial dysfunction and oxidative damage in parkin-deficient mice. *J. Biol. Chem.*, **279**, 18614–18622.
 51. Wood-Kaczmar, A., Gandhi, S., Yao, Z., Abramov, A.Y., Miljan, E.A., Keen, G., Stanyer, L., Hargreaves, I., Klupsch, K., Deas, E. *et al.* (2008) PINK1 is necessary for long term survival and mitochondrial function in human dopaminergic neurons. *PLoS ONE*, **3**, e2455.
 52. Gegg, M.E., Cooper, J.M., Schapira, A.H. and Taanman, J.W. (2009) Silencing of PINK1 expression affects mitochondrial DNA and oxidative phosphorylation in dopaminergic cells. *PLoS ONE*, **4**, e4756.
 53. Chen, Y. and Gibson, S.B. (2008) Is mitochondrial generation of reactive oxygen species a trigger for autophagy? *Autophagy*, **4**, 246–248.
 54. Martindale, J.L. and Holbrook, N.J. (2002) Cellular response to oxidative stress: signaling for suicide and survival. *J. Cell Physiol.*, **192**, 1–15.
 55. Scherz-Shouval, R., Shvets, E., Fass, E., Shorer, H., Gil, L. and Elazar, Z. (2007) Reactive oxygen species are essential for autophagy and specifically regulate the activity of Atg4. *EMBO J.*, **26**, 1749–1760.
 56. Macedo, M.G., Anar, B., Bronner, I.F., Cannella, M., Squitieri, F., Bonifati, V., Hoogeveen, A., Heutink, P. and Rizzu, P. (2003) The DJ-1L166P mutant protein associated with early onset Parkinson's disease is unstable and forms higher-order protein complexes. *Hum. Mol. Genet.*, **12**, 2807–2816.
 57. Chang, N.C., Nguyen, M., Germain, M. and Shore, G.C. (2010) Antagonism of Beclin 1-dependent autophagy by BCL-2 at the endoplasmic reticulum requires NAF-1. *EMBO J.*, **29**, 606–618.
 58. Lutz, A.K., Exner, N., Fett, M.E., Schlehe, J.S., Kloos, K., Lammermann, K., Brunner, B., Kurz-Drexler, A., Vogel, F., Reichert, A.S. *et al.* (2009) Loss of parkin or PINK1 function increases Drp1-dependent mitochondrial fragmentation. *J. Biol. Chem.*, **284**, 22938–22951.
 59. Winklhofer, K.F., Henn, I.H., Kay-Jackson, P.C., Heller, U. and Tatzelt, J. (2003) Inactivation of parkin by oxidative stress and C-terminal truncations: a protective role of molecular chaperones. *J. Biol. Chem.*, **278**, 47199–47208.
 60. Matlib, M.A., Shannon, W.A. Jr and Srere, P.A. (1979) Measurement of matrix enzyme activity in situ in isolated made permeable with toluene. *Methods Enzymol.*, **56**, 544–550.
 61. Kim, R.H., Peters, M., Jang, Y., Shi, W., Pintilie, M., Fletcher, G.C., DeLuca, C., Liepa, J., Zhou, L., Snow, B. *et al.* (2005) DJ-1, a novel regulator of the tumor suppressor PTEN. *Cancer Cell*, **7**, 263–273.
 62. Hyslop, P.A. and Sklar, L.A. (1984) A quantitative fluorimetric assay for the determination of oxidant production by polymorphonuclear leukocytes: its use in the simultaneous fluorimetric assay of cellular activation processes. *Anal. Biochem.*, **141**, 280–286.
 63. Chappell, J.B. and Perry, S.V. (1954) Biochemical and osmotic properties of skeletal muscle mitochondria. *Nature*, **173**, 1094–1095.
 64. Seifert, E.L., Bezaire, V., Estey, C. and Harper, M.E. (2008) Essential role for uncoupling protein-3 in mitochondrial adaptation to fasting but not in fatty acid oxidation or fatty acid anion export. *J. Biol. Chem.*, **283**, 25124–25131.
 65. Reynafarje, B., Costa, L.E. and Lehninger, A.L. (1985) O₂ solubility in aqueous media determined by a kinetic method. *Anal. Biochem.*, **145**, 406–418.